Theoretical and Applied Genetics (2019) 132:2985–2996
https://doi.org/10.1007/s00122-019-03400-6

ORIGINAL ARTICLE

Fine mapping of a silique length- and seed weight-related gene in *Brassica napus*

Wenhao Shen[1] · Pei Qin[1] · Mengjiao Yan[1] · Bao Li[1] · Zengxiang Wu[1] · Jing Wen[1] · Bin Yi[1] · Chaozhi Ma[1] · Jinxiong Shen[1] · Tingdong Fu[1] · Jinxing Tu[1]

Received: 21 March 2019 / Accepted: 11 July 2019 / Published online: 18 July 2019

Abstract

Key message **Using microarray analysis combined with map-based cloning, a major locus positively regulating SL and SW was mapped to a 98.47 kb interval on A09 in rapeseed.**

Abstract In rapeseed, seed yield is closely associated with silique-related traits such as silique length (SL) and seed weight (SW). Previously identified quantitative trait loci (QTLs) revealed that SL and SW are complex traits and many QTLs overlap. However, the genetic characterization of the association between SL and SW is poorly understood. In the present study, a BC_3F_3 near isogenic line developed from a short silique plant and the long silique cultivar 'ZS11' was analyzed to identify the locus related to SL. Map-based cloning indicated that a major locus acting as a single Mendelian factor was mapped to a 98.47 kb region on chromosome A09. BLAST analysis and DNA sequencing showed SNP variations and a fragment replacement in the upstream region of the candidate gene BnaA09g55530D may alter gene expression and influence SL. The results showed that this SL locus may also positively affect SW as well as in the 186 rapeseed accessions identified by the associated markers. Therefore, selecting plants with appropriate SL and developing functional markers for the associated gene could play important roles in the molecular breeding of high-yield rapeseed varieties.

Introduction

Oilseed rape (*Brassica napus* L) is an allotetraploid species formed about 7500 years ago by natural hybridization and genome doubling between turnip rape (*Brassica rapa*) and cabbage (*Brassica oleracea*) (Chalhoub et al. 2014). It is one of the most important sources of plant oil and is cultivated worldwide. Rapeseed provides a healthy vegetable oil for human consumption and a high-protein forage for livestock. It is also a source of renewable energy and can be transformed into biofuel for industrial applications. As the population grows and the need for renewable energy increases, the demand for rapeseed also continues to rise. Therefore, the breeding and cultivation of high-yield rapeseed varieties have become top priorities.

Seed yield is a complex trait that is influenced by various factors (Diepenbrock 2000). Silique length (SL), seed weight (SW), seed number per silique (SS), and siliques per plant (SP) are closely associated with seed yield improvement (Chen et al. 2007; Li et al. 2014). Rapeseed siliques continually supply nutrients from photosynthesis, transport carbohydrates from the vegetative organs to the seeds and ensure normal seed development (Bennett et al. 2011; King et al. 1997; Rossato et al. 2001). Siliques should have large photosynthetic areas, furnish sufficient nutrients, and provide adequate space for the development of the encoded seeds (Chay and Thurling 1989a). SL is closely associated with SW and seed yield, and numerous reports have proved that the incensement of SL could effectively improve seed yield (Chen et al. 2007; Khan et al. 2006; Wang et al. 2016; Sadat et al. 2010; Samizadeh et al. 2007; Udall et al. 2006; Zhang et al. 2011). Chay and Thurling (1989a) discovered that SP varied independently of SL and SW tended to increase with the increasing of SL. Through introgression of

Communicated by Albrecht E. Melchinger.

Electronic supplementary material The online version of this article (https://doi.org/10.1007/s00122-019-03400-6) contains supplementary material, which is available to authorized users.

✉ Jinxing Tu
tujx@mail.hzau.edu.cn

[1] National Key Laboratory of Crop Genetic Improvement, College of Plant Science and Technology, National Sub-Center of Rapeseed Improvement in Wuhan, Huazhong Agricultural University, Wuhan 430070, China

long-pod genes into cultivars with a suitable genetic background would increase seed weight per silique with little or no reduction in SP, there might still be some benefit to select SL in different genetic backgrounds (Chay and Thurling 1989b). The analysis of 112 full-sib families variated in SL indicated that long siliques had more seeds and a greater seed yield per plant with little differences in SP (Diepenbrock 2000). SL and SW showed similar high heritability, and the variations in SL were more likely to be the cause of the distinction in SW (Li et al. 2014). Thus, long silique is an appropriate feature in rapeseed breeding programs. Previous studies have confirmed that SL and SW are controlled by multiple gene loci. Several quantitative trait loci (QTLs) have been identified in *B. napus* through traditional genetic mapping and association studies (Chen et al. 2007; Dong et al. 2018; Fan et al. 2010; Fu et al. 2015; Li et al. 2014; Shi et al. 2009; Wang et al. 2016; Yang et al. 2012; Zhang et al. 2011). Several SL and SW QTLs have been found to be overlapped or linked on chromosomes A04, A09, C06, and C08 (Dong et al. 2018; Fu et al. 2015; Li et al. 2014).

Analysis of the loci related to SL and SW can elucidate the genetic mechanism of silique development and the improvement of rapeseed yield. A recent study revealed that the nuclear gene *BnaA.ARF18.a* on chromosome A09 affects both SL and SW development in rapeseed (Liu et al. 2015). Functional markers for this gene were developed to distinguish the optimal alleles governing SL and SW in A09 (Dong et al. 2018). However, SW selection in the field is difficult since SW can only be calculated after harvest and the recognized QTLs cannot yet be applied in high-yield rapeseed breeding. In this study, a major locus in *B. napus* acting as a single Mendelian SL-controlling factor was narrowed down to a 98.47 kb interval on A09 using a *Brassica* 60 K Illumina Infinium™ SNP array and a map-based cloning strategy. The SW could also be improved in individuals expressing high levels of this candidate gene locus. The relationship between SL and SW was also demonstrated in the 186 rapeseed accessions identified by the associated markers. These results provide a strategy for oil rapeseed improvement by selecting for appropriately long siliques. The corresponding locus and its functional markers may then be used in the cultivation of high-yield rapeseed varieties.

Materials and methods

Plant materials, population development, and trait measurements

A *B. napus* doubled haploid line 'DH46' achieved from the doubled haploid lines of the recurrent population (Zhao et al. 2016) and the conventional cultivar 'ZS11' were used as parents in this study, and they were provided by the Rapeseed Laboratory of Huazhong Agricultural University. 'DH46' exhibited short siliques and low SS, was crossed with 'ZS11' to produce a F_1 generation. The F_1 plants were backcrossed with the recurrent parent 'DH46' (as the male) three times without any selections to construct a mapping population, BC_3F_1. A BC_3F_1 subpopulation obtained from one BC_2F_1 plant was selected, which consisted of 236 individuals having SL variations with a 1:1 segregation ratio, and was used to locate the SL-related gene. To generate fine mapping of the *BnSLA09* gene, the long-silique BC_3F_1 plants were self-pollinated to produce a BC_3F_2 population. Since the SS could influence silique-related traits, only individuals with no fertility problems and heterozygous locus of *BnSLA09* in BC_3F_2 population were self-pollinated to develop 4824 lines of a BC_3F_3 population. Plants with a homozygous locus of *BnSLA09* originating from 'ZS11' and 'DH46' were identified from the BC_3F_3 population and named L-NIL and S-NIL, respectively. Both the SL and SS for each plant among the BC_3F_3 generation were estimated based on the average length of ten well-developed siliques (not including the pod beak) from the middle of the main inflorescence. The weight of 1000 fully filled open-pollinated seeds was measured and represented the SW of each individual.

Histological observation

After 20 days of flowering, long and short siliques from the BC_3F_3 plants were sampled and fixed in FAA solution (50% ethanol, 5% glacial acetic acid, and 5% formaldehyde) for 24–48 h. The fixed materials were dehydrated in an ethanol series (60, 70, 80, 90, and 100%), vacuum-dried, and coated with gold under vacuum. The outer surfaces of the siliques were observed under a JSM-6390LV scanning electron microscope (JEOL Ltd., Akishima, Tokyo, Japan) at an accelerating voltage of 10 kV.

DNA extraction and bulked segregant analysis (BSA)

Genomic DNA of all accessions was extracted from fresh leaf tissues using a modified cetyltrimethylammonium bromide (CTAB) method (Murray and Thompson 1980). For the *Brassica* 60 K Illumina Infinium™ SNP array analyses, BC_3F_1 plants were randomly selected to construct DNA bulks. The DNA from forty long- and forty short-silique plants was extracted using a DNA Secure Plant Kit (DP320, Tiangen Biotech, Beijing, China) then randomly pooled with an equivalent amount of DNA to construct four long- and four short-silique pools (L-pools and S-pools, respectively). All DNA pools were adjusted to 100 ng/μl before the SNP array analysis.

SNP analysis

A *Brassica* 60 K Illumina Infinium™ SNP array contained 52,157 markers suitable for the allotetraploid *Brassica napus* (Clarke et al. 2016). The SNP analysis was performed according to the methodology detailed in Xu et al. (2016). Scanned SNPs differing between the four L-pools and the four S-pools were considered candidate gene regions associated with SL. The retained SNPs were used in a BLAST search against the *B. napus* 'ZS11' genome database (https://www.ncbi.nlm.nih.gov/assembly/GCF_000686985.2) to locate the chromosome positions (*E* value ≤ '1e−12'). SNPs matched to multiple loci in the genome were removed, and only the top blast hits were retained for further analysis.

Development of single sequence repeat (SSR) and InDel markers

According to the results of the SNP analysis, partial sequences of *B. napus* 'ZS11' A09 chromosome were selected to develop SSR markers in WebSat (http://wsmartins.net/websat/). Multiple insertions/deletions among the candidate regions were found by comparing the resequencing data of 'DH46' (unpublished) with *B. napus* 'ZS11' genome sequences. InDel markers were designed with Primer 3 (http://primer3.ut.ee/). All primers were used to amplify genomic DNA from the two parents and the L-pools and S-pools via a standard PCR as described by Xia et al. (2012). The PCR products were detected on 6% denaturing polyacrylamide gels, and only polymorphic markers were selected to narrow down the interval in the BC_3F_3 population.

Genetic mapping of the *BnSLA09* locus

The 236 BC_3F_1 and 4824 BC_3F_3 individuals were used to construct a rough initial linkage map and a fine map of the *BnSLA09* locus, respectively. Segregation data associated with polymorphic SSR and InDel markers linked to the gene were analyzed with JoinMap® 4 and MapDraw (Liu and Meng 2003; Van Ooijen 2006). All genetic distances (cM) were counted with Kosambi's mapping function (Kosambi 1944).

Analysis of the genes in the mapping interval of the *BnSLA09* locus

All putative genes with their annotation information in the target interval were obtained from the *B. napus* 'ZS11' (https://www.ncbi.nlm.nih.gov/assembly/GCF_000686985.2) and *B. napus* 'Darmor-*bzh*' (http://www.genoscope.cns.fr/brassicanapus/data/) genome databases. The orthologous genes were identified by BLAST analysis in the online Arabidopsis databases (TAIR, http://www.arabidopsis.org/), and only the top blast hits were considered. A bioinformatics analysis of all genes within the *BnSLA09* locus region was performed for candidate gene predication. Promoter- and full-length genomic sequences of the candidate gene were amplified and sequenced between the two parents and the BC_3F_3 individuals.

RNA extraction and quantitative real-time PCR (qRT-PCR)

At the flowering stage, four different samples (L1: 0–2 mm buds; L2–L4: 2–4, 4–6, and 6–8 mm pistils of buds) were taken from BC_3F_3 individuals with long and short siliques and frozen in liquid nitrogen, and three biological replicates were used. Total RNA was isolated with a Universal Plant Total RNA Extraction Kit (RP3302; BioTeke Corporation, Beijing, China) according to the manufacturer's instructions. A total of 2 μg RNA was reverse transcribed into cDNA with TransScript One-Step gDNA Removal and cDNA Synthesis SuperMix (TransGen Biotech, Beijing, China) and Oligo(dT)18 primer following the manufacturer's instructions. Real-time PCR was performed in triplicate for each sample using the TransStart Tip Green qPCR SuperMix (TransGen Biotech, Beijing, China) on a CFX96 Real-Time System (Bio-Rad Laboratories, Inc., Hercules, CA, USA). The gene-specific primers used in the amplification are listed in Table S2, and the reference gene primers used for relative quantification and the analytical method are described in Zhou et al. (2012).

Results

Phenotypic description of 'DH46'

The 'DH46' cultivar used in the present study was obtained from the doubled haploid lines of the recurrent population (Zhao et al. 2016) with short siliques and low SS. In the flowering stage, there were no obvious differences between 'DH46' and the conventional cultivar 'ZS11' in terms of the main inflorescence and the pollen, but their silique traits substantially differed (Fig. 1, Fig. S1). Most 'DH46' siliques had no seeds and dropped at the initial flowering stage; several siliques yielded a few seeds at maturity (Fig. 1b). For 'DH46,' the average SL was 1.50 ± 0.14 cm and the average SS was 1.13 ± 0.06; these values were significantly lower ($P < 0.001$) than those for 'ZS11' (8.07 ± 1.06 cm and 23.96 ± 0.10, respectively) (Fig. 1c).

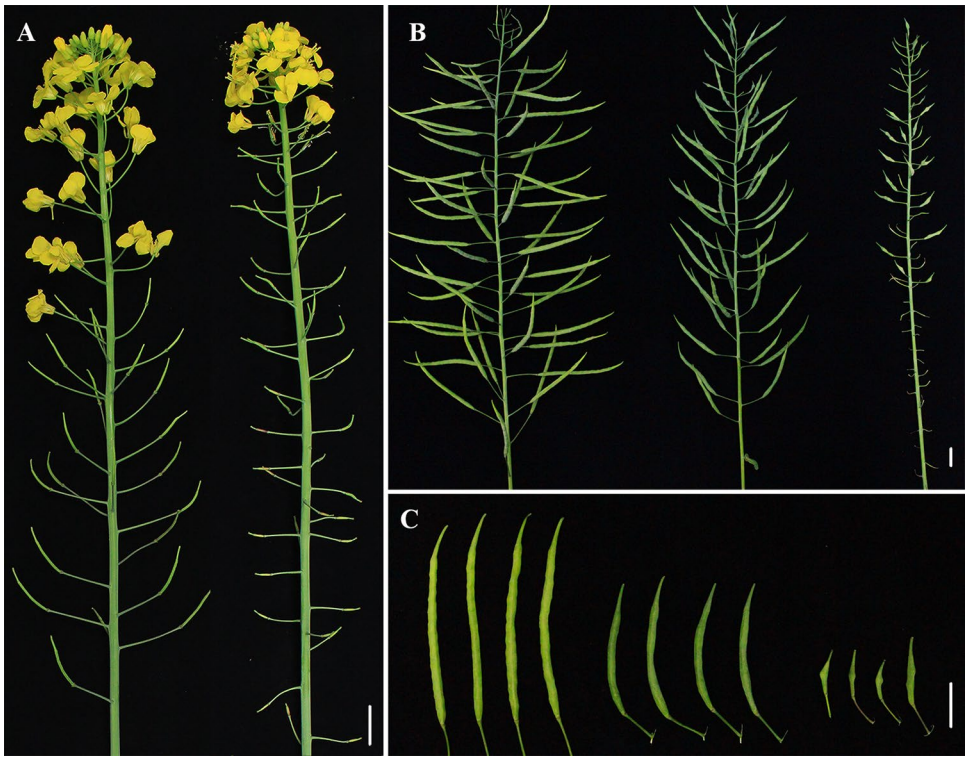

Fig. 1 Phenotypes of flowers and siliques in *B. napus*. **a** Main inflorescence of 'ZS11' (left) and 'DH46' (right) at flowering stage. **b**, **c** Main inflorescence and siliques of 'ZS11,' F1 hybrid of 'ZS11' × 'DH46' and 'DH46' at mature stage (from left to right). Bars, 2 cm

Genetic characterization

The F_1 generation was constructed by crossing 'ZS11' with the male parent 'DH46,' as 'DH46' produced few seeds but normal pollen (Fig. S1). The F_1 plants exhibited an intermediate phenotype with average SL and SS of 5.39 ± 0.23 cm and 6.31 ± 0.04, respectively. The SS can influence SL, but it was still easy to distinguish between long and short siliques within the mapping population because the former had longer and sharper pod beaks than the latter. The siliques of all F_1 plants were considered long because their pod beaks were long and pointed (Fig. 1c). Compared to SL, SS was found to be a more complex trait in the mapping population (data not shown); thus, we focused on variations in SL in the next analysis.

The F_1 individuals were backcrossed with the recurrent parent 'DH46' (as the male) to generate the advanced backcross lines. The short silique of 'DH46' was mainly due to the less SS, and SL variations among the mapping populations were ignored. However, in the BC_3F_1 generation, except the SS difference, the variations in SL were noticed in many BC_3F_1 progenies. A progeny of one BC_2F_1 plant comprising 236 BC_3F_1 individuals was analyzed and found to consist of 120 long-silique plants and 116 short-silique plants (according to their pod beaks). A *Chi-square* test indicated that the segregation ratio was nearly 1:1 (Table 1). To exclude the effects of SS on SL, only plants in the BC_3F_2 generation with no seed development defects and heterozygous locus of *BnSLA09* were self-pollinated to construct a BC_3F_3 population (Fig. S2a). The BC_3F_3 progeny segregated in a 3:1 ratio (Table 1); therefore, SL is controlled by a single nuclear gene locus.

Table 1 Genetic analyses of the silique trait in F1, BC_3F_1 and BC_3F_3 progenies

Generations	Total	Long silique	Short silique	Expected ratio	*Chi-square* value
F_1	58	58	0		
BC_3F_1	236	120	116	1:1	0.04
BC_3F_3	4824	3627	1197	3:1	0.08

Chi-square test, $\chi^2_{0.05,1} = 3.84$

SNP analysis

A *Brassica* 60 K Illumina Infinium™ SNP array was used to screen the L- and S-pools from the BC_3F_1 population, and 32 different SNPs were found after filtering. A BLAST search against the *B. napus* 'ZS11' genome database was performed, and only 16 SNPs remained. Fourteen SNPs were localized to the A09 chromosome, and one each was located in A03 and C06 (Table 2). The SNPs in A09 were localized mainly in a concentrated region between 36.32 and 38.53 Mb. This finding revealed that the target gene

Table 2 Distribution of retained SNPs against the *B. napus* cv. 'ZS11' genome

SNP id	Chromosome	Start site	End site	Alignment length	Identity (%)	*E* value
Bn-A09-p4895204	A03	8,569,888	8,569,937	50	100	3e−20
Bn-A09-p4997670	A09	6,151,356	6,151,307	50	96	2e−15
Bn-A09-p5037318	A09	6,207,996	6,207,947	50	98	1e−13
Bn-A09-p29756068	A09	36,324,008	36,324,057	50	100	3e−20
Bn-A09-p29944855	A09	36,508,262	36,508,213	50	100	3e−20
Bn-A09-p30257404	A09	36,807,405	36,807,356	50	100	3e−20
Bn-A09-p30284813	A09	36,834,817	36,834,768	50	100	3e−20
Bn-A09-p30329663	A09	36,882,921	36,882,873	50	98	2e−15
Bn-A09-p25899239	A09	37,013,860	37,013,811	50	100	3e−20
Bn-A09-p30439085	A09	37,116,215	37,116,166	50	100	3e−20
Bn-A09-p31377029	A09	38,231,860	38,231,811	50	100	3e−20
Bn-A09-p31554401	A09	38,420,928	38,420,879	50	100	3e−20
Bn-A09-p31613718	A09	38,530,144	38,530,193	50	100	3e−20
Bn-A09-p31614055	A09	38,530,583	38,530,534	50	100	3e−20
Bn-A09-p31614376	A09	38,530,904	38,530,855	50	100	3e−20
Bn-scaff_18439_1-p627420	C06	15,791,828	15,791,877	50	100	3e−20

controlling the SL phenotype is located in ~ a 2.21 Mb interval within A09 and named *BnSLA09*.

Fine mapping of the *BnSLA09* gene

SSR and InDel markers were designed to fine map the *BnSLA09* gene based on the 2.21 Mb candidate region of the *B. napus* 'ZS11' genome. Among the 19 polymorphic SSR markers, only five primer pairs with legible and steady bands were selected to analyze the 236 individuals from the BC_3F_1 population. SSR1253 and SSR1270 were closely linked to the *BnSLA09* gene locus at genetic distances of 2.12 and 1.70 cM, respectively. To narrow the region of the *BnSLA09* gene, several InDel markers between the SSR1253 and SSR1270 intervals were designed and 4824 plants of the BC_3F_3 generation were screened. Recombinant numbers indicated that the SSR1253, SSR1259, In1-18, and In1-19 markers were located on one side of *BnSLA09*, whereas the In2-52, In1-27, In1-34, and SSR1270 markers were located on the other side. In2-37 and In1-22 were co-segregated markers linked with *BnSLA09* (Fig. 2). *BnSLA09* was eventually localized between In1-19 and In2-52 which corresponded to ~ 98.47 kb on chromosome A09 in the *B. napus* 'ZS11' genome.

Biological roles of *BnSLA09*

To elucidate the functions of *BnSLA09*, silique-related traits and the outer cells of young siliques were investigated in L-NIL and S-NIL plants of the BC_3F_3 generation. SL and SW both significantly differed between the L-NIL and S-NIL plants in the two environments and were on average 61.3% and 24.5% larger in the long-silique plants than in the short-silique plants, respectively (Table 3; Fig. 3). Consistent with the SW data, the seeds in the L-NIL plants were much larger than those in the S-NIL plants (Fig. 3e, f). Scanning electron microscopy (SEM) revealed that the outer cells of the L-NIL siliques were much longer than those of the S-NIL siliques (Fig. 3c, d). Long siliques have a comparatively large photosynthetic area and can provide more nutrients and space for encoded seed development. Therefore, the variation in SL controlled by *BnSLA09* is influenced by silique cell wall elongation. The relatively larger silique surface area in L-NIL plants can provide much more photosynthetic product and increase SW to a greater extent than S-NIL plants.

Candidate gene identification

The target region of *BnSLA09* was analyzed based on the *B. napus* 'ZS11' and 'Darmor-*bzh*' genomes. The putative functions of these genes were adopted from their orthologs in *A. thaliana*. The candidate interval contained 14 predicted genes in the *B. napus* 'ZS11' genome and corresponding to 13 genes in the *B. napus* 'Darmor-*bzh*' genome (Fig. 2; Table 4). An annotation analysis of these genes indicated that BnA09g0377760.1/BnaA09g55530D was highly orthologous to AT3G61880 in *Arabidopsis*. AT3G61880, also known as *CYP78A9*, encodes a cytochrome P450 monooxygenase. Compared to the wild type, mutants of this gene exhibit short pods and small seeds, whereas overexpressing lines have long siliques and large seeds (Ito and Meyerowitz 2000; Sotelo-Silveira et al. 2013). BnA09g0377780.1/

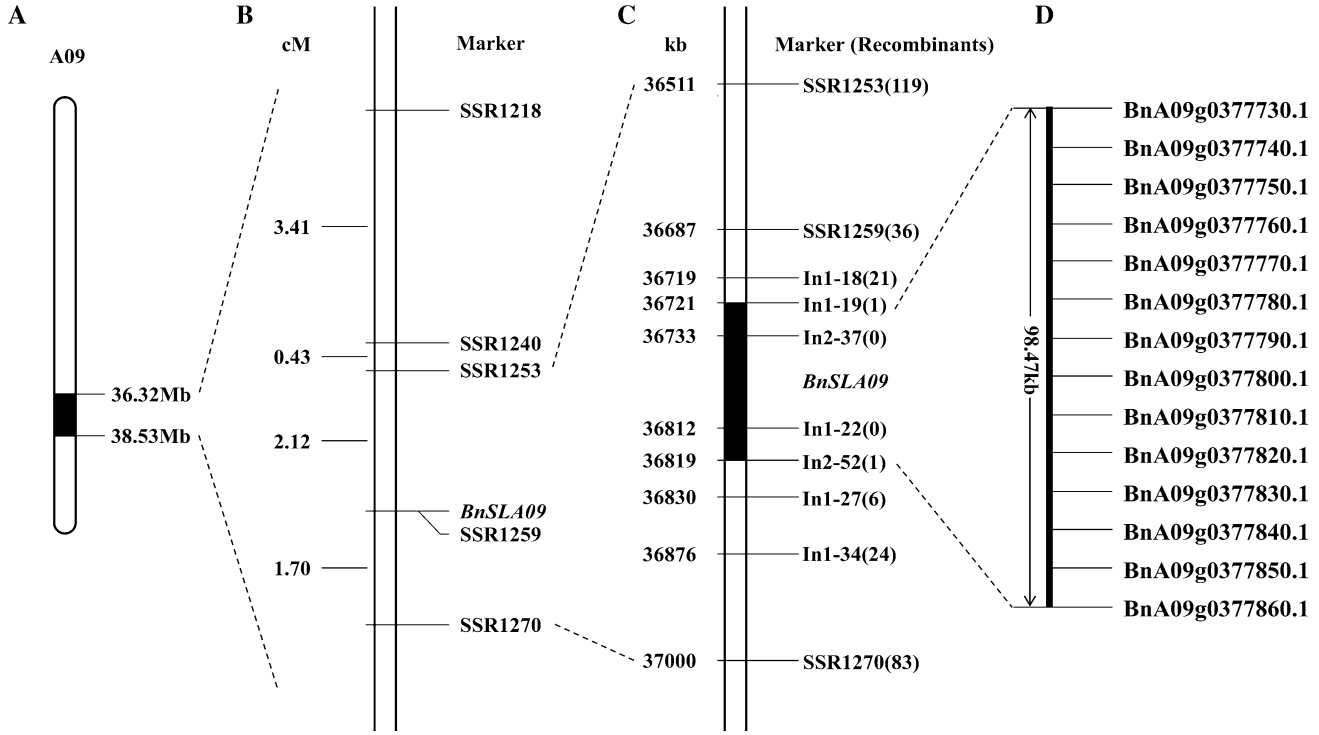

Fig. 2 Mapping of the silique length locus in *B. napus*. **a** Physical map of candidate region on A09 chromosome in *B. napus*. **b** Partial genetic map of the *BnSLA09* interval, developed from the BC_3F_1 generation. **c** Particle linkage map of the *BnSLA09* region from the BC_3F_3 population. **d** Candidate region of *BnSLA09* gene locus and the annotated genes in the reference genome of 'ZS11.' Sequences of molecular makers are listed in Table S1. More detailed information of these genes is listed in Table 4

Table 3 Statistical data of silique-related traits of BC_3F_3 from two environments

Environment	Genotype	SL (cm)	SS	SW (g/1000 seeds)
Wuhan	L-NIL	7.82 ± 0.39***	21.00 ± 2.30	3.81 ± 0.48**
	S-NIL	4.40 ± 0.36	20.12 ± 2.35	2.98 ± 0.50
Lanzhou	L-NIL	8.57 ± 0.61***	23.49 ± 2.85	3.50 ± 0.43**
	S-NIL	5.76 ± 0.58	22.13 ± 2.22	2.89 ± 0.33

***Significantly different at $P < 0.001$; **significantly different at $P < 0.01$

BnaA09g39470D is orthologous to AT3G61900, which is also known as the *SAMLL AUXIN UP RNA33* (*SAUR33*) gene. It belongs to the SAUR-like auxin-responsive protein family which is one of three primary auxin-induced gene families in *Arabidopsis*. The function of *SAUR33* is unclear, but it was reported that *SAUR41* regulates cell expansion by auxin modulation and *SAUR63* promotes hypocotyl and stamen filament elongation (Chae et al. 2012; Kong et al. 2013). Both of these genes in the candidate region may contribute to the variations in SL, and so we focused on them in the subsequent investigations.

To determine which gene is responsible for SL differentiation, the relative expression levels of both genes were evaluated during early silique development in BC_3F_3 L-NIL and S-NIL plants. The expression levels of BnaA09g39470D did not significantly differ between the L-NIL and S-NIL individuals at the L1, L2, and L4 stages, and the only difference was at the L3 stage (Fig. 4a). However, the transcript levels of BnaA09g55530D were significantly higher in L-NIL than S-NIL plants during early silique development, especially at the L3 and L4 stages (Fig. 4b). The high expression level of BnaA09g55530D produced long siliques and large seeds in L-NIL matched the phenotype of its orthology in *Arabidopsis* (Ito and Meyerowitz 2000; Sotelo-Silveira et al. 2013). Therefore, we concluded that BnaA09g55530D was the most likely candidate gene for *BnSLA09* and named it '*BnaA.CYP78A9.a*' based on the standard nomenclature of Østergaard and King (2008).

Since *B. napus* is an allotetraploid species, homologs of *BnaA.CYP78A9.a* were identified by BLAST analysis in the reference genome of *B. napus* 'Darmor-*bzh*.' In brief, BnaA04g00510D on chromosome A04, BnaC08g31760D

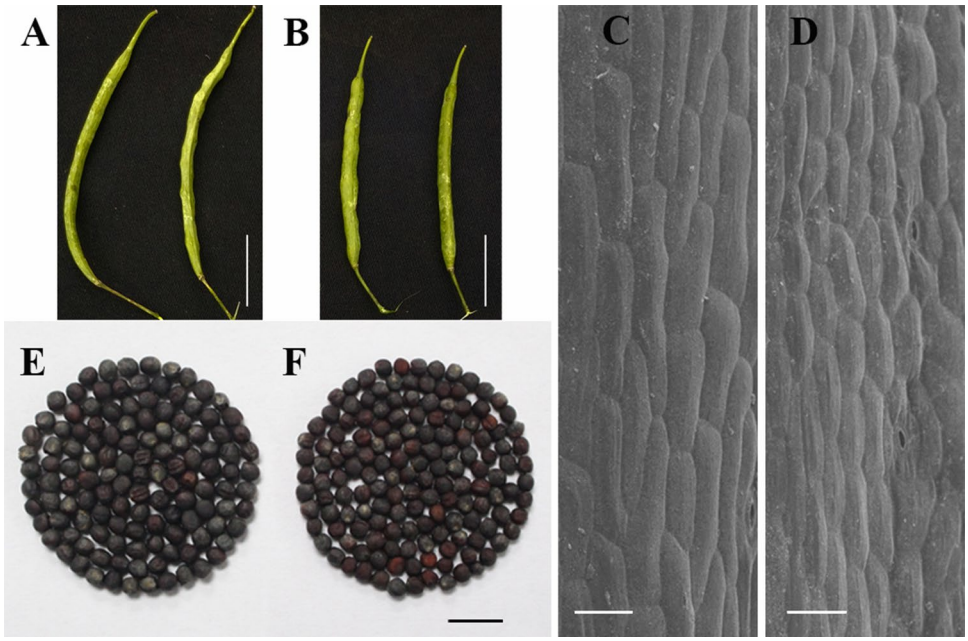

Fig. 3 Phenotypes of silique-related traits in L-NIL and S-NIL plants in BC_3F_3 generation. **a**, **b** Comparison of the silique morphology in L-NIL (**a**) and S-NIL (**b**) plants. Bars, 2 cm. **c**, **d** Scanning electron microscope images of the outer cells of siliques in L-NIL (**c**) and S-NIL (**d**) plants, respectively. Bars, 50 µm. **e**, **f** Comparison of seeds in L-NIL (**e**) and S-NIL (**f**) plants. Bar, 0.5 cm

Table 4 Prediction and annotation of candidate genes within the mapping region

Gene of *B. napus*	Chromosome position	Orthologous gene of *A. thaliana*	Annotation
BnA09g0377730.1/BnaA09g55560D	36725350–36730532	AT2G46620	P-loop containing nucleoside triphosphate hydrolases superfamily protein
BnA09g0377740.1/BnaA09g55550D	36734365–36736067	AT3G61870	Plant/protein
BnA09g0377750.1/BnaA09g55540D	36736541–36737230	AT2G46630	Serine/arginine repetitive matrix protein
BnA09g0377760.1/BnaA09g55530D	36740578–36742333	AT3G61880	Encodes a cytochrome P450 monooxygenase
BnA09g0377770.1	36777661–36778131	AT5G63200	Tetratricopeptide repeat (TPR)-containing protein
BnA09g0377780.1/BnaA09g39470D	36781953–36782619	AT3G61900	SAUR-like auxin-responsive protein family
BnA09g0377790.1/BnaA09g39480D	36785670–36786981	AT3G61910	NAC transcription factor NST2
BnA09g0377800.1/BnaA09g39490D	36794060–36794626	AT3G61920	UvrABC system protein C
BnA09g0377810.1/BnaA09g39500D	36797252–36797584	AT3G61930	Hypothetical protein
BnA09g0377820.1/BnaA09g39510D	36799427–36800522	AT3G61940	Member of Zinc transporter (ZAT) family
BnA09g0377830.1/BnaA09g39520D	36801997–36803142	AT3G61950	MYC-type transcription factor
BnA09g0377840.1/BnaA09g39530D	36803204–36807083	AT3G61960	Protein kinase superfamily protein
BnA09g0377850.1/BnaA09g39540D	36815290–36816168	AT3G61970	AP2/B3-like transcriptional factor family protein
BnA09g0377860.1/BnaA09g39550D	36818814–36819625	AT3G61980	Encodes a Kazal-type serine proteinase inhibitor

on chromosome C08, and BnaCnng73170D on chromosome Cnn were recognized as homoeologs (Glover et al. 2016) and their expression levels were measured in the early silique development stages. The expression levels of these three genes in both parents were extremely low compared with that of *BnaA.CYP78A9.a* in L-NIL plants (Fig. S3). Therefore, the long-silique phenotype in L-NIL plants was the result of the overexpression of *BnaA.CYP78A9.a*.

To characterize the relationship between the candidate gene and the variations in the silique-related traits, the promoter sequences, full-length genomic DNA, and coding sequences of *BnaA.CYP78A9.a* in 'ZS11' and 'DH46' were amplified. DNA sequencing revealed that the entire gene and coding sequences of *BnaA.CYP78A9.a* (GenBank accession number: MK224591 and MK224590) in 'ZS11' and 'DH46' were consistent with the reference sequences in the *B. napus* 'ZS11' genome. This gene consisted of two exons with an encoded protein composed of 532 amino acids, and four SNPs in the promoter interval (~ 3.0 kb before the start codon) between the two parents were found (Fig. 5). Moreover, a ~ 12.4 kb DNA sequence, ~ 3.9 kb upstream of the transcription initiation

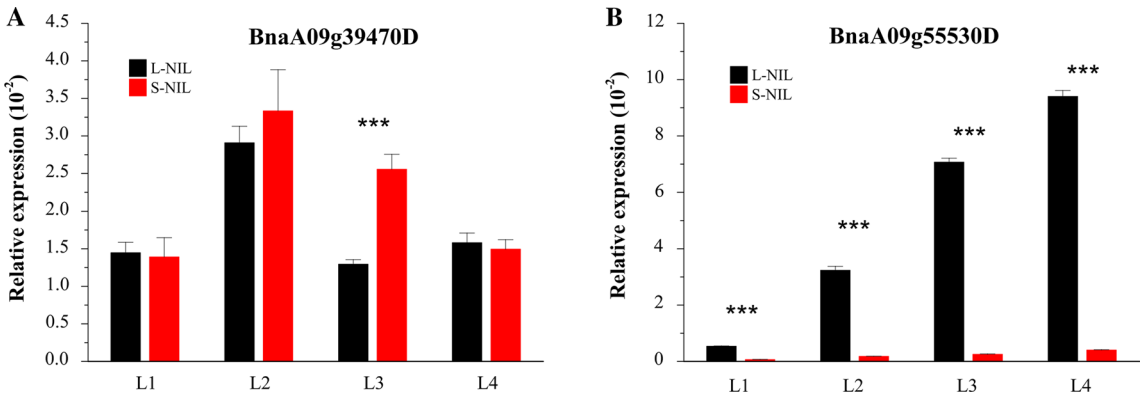

Fig. 4 Relative expression of candidate genes BnaA09g39470D (**a**) and BnaA09g55530D (**b**) at different silique development stages between L-NIL and S-NIL plants. L1: 0–2 mm buds; L2–L4: 2–4, 4–6, and 6–8 mm pistils of buds. ***Significantly different at $P < 0.001$

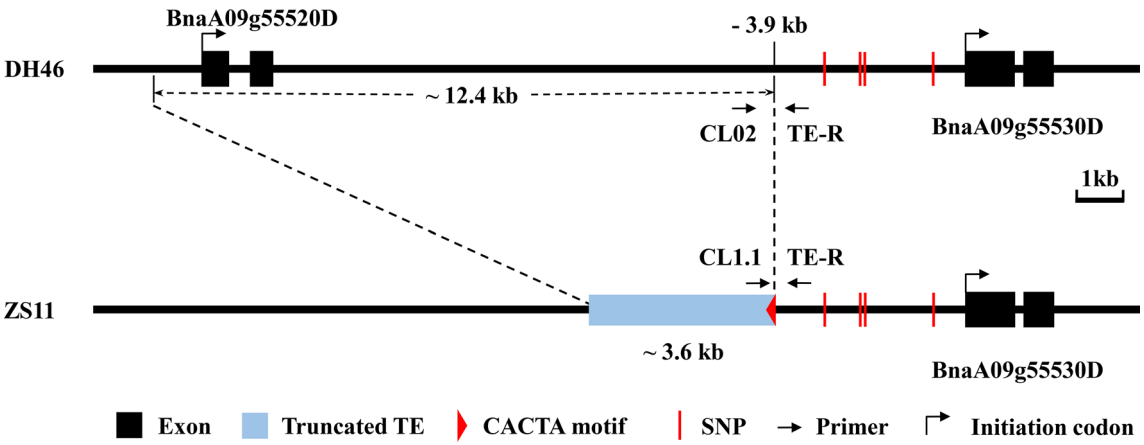

Fig. 5 Gene structure, SNP variations, and fragment replacement between 'ZS11' and 'DH46'; horizontal black arrows represent co-segregation analysis primers

codon of *BnaA.CYP78A9.a* in 'DH46,' was replaced by a ~ 3.6 kb fragment in 'ZS11' (Fig. 5). In the corresponding regions, the 12.4 kb DNA sequence in 'DH46' resembled the reference genome sequence of *B. napus* 'Darmor-*bzh*,' whereas the 3.6 kb fragment in 'ZS11' was similar to the *B. napus* 'ZS11' genome sequence. The 3.6 kb fragment had a CACTA sequence in its reverse 3' end which might have been a CACTA transposable element (TE). Therefore, we performed a sequence analysis in the public database CENSOR (www.girinst.org/censor/index.php). The replaced fragment was probably part of the *BRENSPM1* element belonging to the CACTA transposon family, but its 5' end was missing mainly because of the imprecise excision of an entire transposon (Fig. 5). The 12.4 kb DNA fragment in 'DH46' contained the putative gene BnaA09g55520D which is orthologous to AT3G61890 (*ATHB12*) in *Arabidopsis* and may positively control cell enlargement and expand leaves (Hur et al. 2015).

Development of functional markers to identify different SL in *B. napus*

Based on the fragment replacements in 'ZS11' and 'DH46,' two pairs of functional markers were designed to identify long- and short-silique plants (Fig. 5). The CL1.1 and TE-R primer pair yielded a specific amplification product of 801 bp in 'ZS11' (Fig. 6a), while the CL02 and TE-R primer pair generated a unique 1024 bp product in 'DH46' (Fig. 6b). Amplification of the BC_3F_3 plants with these primers resulted in consistent silique phenotypes (Fig. 6). Therefore, these primers were highly effective at distinguishing the variations in SL between the two parents and their progenies.

To verify the relationship of these co-segregation markers with SL and SW in *B. napus*, the primers were used to screen a diversity panel as described by Liu et al. (2016).

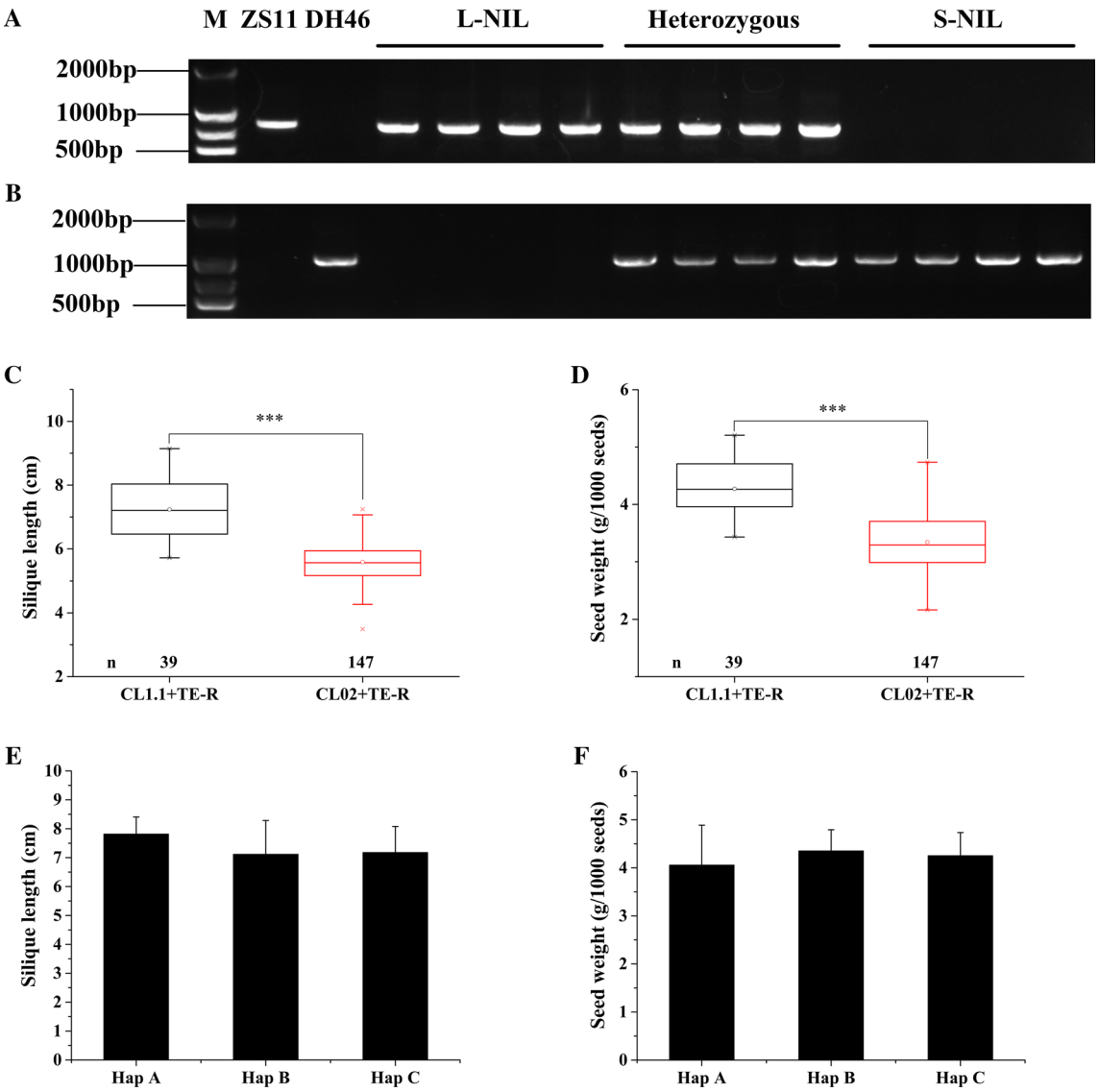

Fig. 6 Co-segregation analysis of long- and short-silique plants and silique traits in the identified accessions. **a** Primer CL1.1 and TE-R, the product is 801 bp. **b** Primer CL02 and TE-R, the product is 1024 bp. **c**, **d** Box plots for silique length (**c**) and seed weight (**d**) of identified accessions in the 521 natural population. The *middle line*, the median, the *outer dots*, the mean, the *box*, the range of the 25th to 75th percentiles of the total data, the *cross*, the max and min data, and the *vertical lines*, the interquartile range. Average SL (**e**) and SW (**f**) of three haplotypes of *BnaA.ARF18.a* in the accessions identified by primers CL1.1 and TE-R. ***Significantly different at $P < 0.001$

Among 521 *B. napus* cultivars and inbred lines, 39 accessions were distinguished by the CL1.1 and TE-R primer pair and 147 accessions were identified by the CL02 and TE-R primer pair (Table S3). Analyses of the SL and SW measured in three environments of these accessions showed that SL and SW identified by the CL1.1 and TE-R primer pair were significantly greater than those distinguished by the CL02 and TE-R primer pair (Fig. 6c, d). Therefore, the functional markers designed in our study could be used to discriminate *B. napus* plants with different SL and SW.

The effect of *BnaA.CYP78A9.a* on SL and SW variations in *B. napus*

The candidate gene *BnaA.CYP78A9.a* and the reported gene *BnaA.ARF18.a* (Liu et al. 2015) are very close on chromosome A09 according to the reference genome of *B. napus* 'ZS11.' In order to figure out the effect of these two genes on SL and SW variations, the haplotypes (Hap A, Hap B, Hap C) of *BnaA.ARF18.a* in our natural populations were analyzed based on the results of Dong et al. (2018). A pair of specific primers (Hap-F, Hap-R) was designed to amplify the critical part of *BnaA.ARF18.a* to distinguish

the haplotypes of them. The sequenced results revealed that only three accessions (accession name: 880101, 2012-9323 and Zhongshuang5) were Hap A, ten accessions were Hap B and other 25 accessions were belonged to Hap C in the 39 accessions identified by the CL1.1 and TE-R primer pair accessions. Moreover, more than 50 accessions classified into Hap A were recognized among the 147 accessions identified by the CL02 and TE-R primer pair. These results indicated that the truncated TE in front of *BnaA.CYP78A9.a* and the Hap C of *BnaA.ARF18.a*, as well as the disappeared TE in front of *BnaA.CYP78A9.a* and the Hap A of *BnaA.ARF18.a*, are closely linked to control SL and SW in most rapeseed varieties.

In addition, the average SL of the three Hap A accessions among the 39 accessions was 7.82 ± 0.59 cm and the average SW was 4.06 ± 0.83 g, which had no significant difference compared to the Hap B or the Hap C accessions among them (average SL was 7.12 ± 1.17 cm and 7.18 ± 0.90 cm; average SW was 4.35 ± 0.44 g and 4.25 ± 0.48 g, respectively) (Fig. 6e, f). Although only a small number of these special accessions were discovered, we could conclude from the existing results that the strong effect of *BnaA.CYP78A9.a* on SL and SW was independent of the haplotypes of *BnaA.ARF18.a* in the 39 accessions identified by the functional markers, which revealed that only the functional copy of *BnaA.CYP78A9.a* was enough to improve the SL and SW in *Brassica napus*.

Discussion

In oilseed rape, SL and SW are important agronomic traits related to crop yield. Only a few QTLs have been identified, and the functional genes controlling these traits are largely unknown. In this study, a DH line 'DH46' with few seeds and short siliques was investigated to map the gene associated with SL. A genetic analysis revealed that variation in the SL was controlled by a single Mendelian factor among the mapping populations, which was narrowed down to a 98.47 kb interval on chromosome A09 by microarray analysis and a map-based cloning strategy. Expression analyses and DNA sequencing showed that BnaA09g55530D, a ortholog of the *Arabidopsis CYP78A9* gene, may control both SL and SW.

Previous studies have shown that several QTLs affecting SL and SW are linked or overlapped, and the major QTLs on chromosome A09 controlling both traits have been identified (Fu et al. 2015; Yang et al. 2012). The candidate gene recognized in the present study is located in this interval; thus, our mapping results are reliable. Moreover, the candidate gene *BnaA.CYP78A9.a* is close to the reported gene *BnaA.ARF18.a* (Liu et al. 2015) and can also affect both SL and SW development in rapeseed. So in the breeding process, we can select plants with this functional locus to achieve suitably long siliques and improve crop yield. *CYP78A9* overexpressing lines in *Arabidopsis* have long siliques, large seeds, and few seeds (Ito and Meyerowitz 2000; Sotelo-Silveira et al. 2013), indicating that high *CYP78A9* expression levels may affect silique-related traits. These findings are consistent with the expression levels of this candidate gene and phenotypes of SL and SW in L-NIL and S-NIL plants. However, the SS in L-NIL plants with overexpressed *CYP78A9* levels is normal. This is mainly due to the expression of *BnaA.CYP78A9.a* homoeologs are at normal levels, and only the gene on chromosome A09 is overexpressed (Fig. 4b, Fig. S3). A recent transcriptome analysis of large and small seeds in rapeseed showed that BnaA09g55530D is upregulated in long-silique plants with large seeds (Li et al. 2018). Moreover, SL and SW are overlapped in the 186 rapeseed accessions identified by the co-segregation markers. This discovery confirms that BnaA09g55530D is the candidate gene responsible for the SL and SW variations observed in this study.

Regulatory elements in the upstream regions of functional genes play important roles in the regulation of gene expression (Kolovos et al. 2012; Porto et al. 2014). Several functional enhancers, silencers, and SNPs have been identified in plants such as a 12 bp enhancer of *NOG1*, an 18 bp silencer of *FZP* in rice (Bai et al. 2017; Huo et al. 2017), a SNP33 located in the promoter region of *bsr-d1* in rice (Li et al. 2017), a *Tourist-like* MITE insertion in the upstream region of *BnFLC.A10* in rapeseed (Hou et al. 2012), and a truncated TE in the upstream region of *HaCYC2c* in sunflower (Chapman et al. 2012). The genomic region of BnaA09g55530D is identical in both parents, and there are only four SNPs and a fragment replacement in the upstream region of the candidate gene (Fig. 5). Among the four *CYP78A9* homoeologs in L-NIL and S-NIL plants, only the *BnaA.CYP78A9.a* in L-NIL plants is overexpressed. Moreover, the functional markers used in the natural population were designed based on the exist of the truncated TE fragment. The accessions identified by primer CL1.1 and TE-R had longer SL and heavier SW than the ones recognized by the primer CL02 and TE-R. Therefore, the truncated TE in the upstream region of *BnaA.CYP78A9.a* in L-NIL plants may upregulate *BnaA.CYP78A9.a* and produce longer siliques and heavier seeds than those of the S-NIL plants.

Silique-related traits have complex relationships, and SS and SW are positively controlled by SL (Chen et al. 2007; Fu et al. 2015; Zhang et al. 2011). Differences in SL between the parental 'DH46' and the S-NIL plants in the BC_3F_3 population are caused mainly by variations in the SS. Since SL and SS are significantly correlated, it is necessary to eliminate the influence of the latter when fine mapping the SL gene locus in the BC_3F_3 population.

With the rapid development of microarray and high-throughput sequencing technologies, there has been a continuous increase in the numbers of rapeseed SNP arrays and reference genomes being exploited (Chalhoub et al. 2014; Clarke et al. 2016; Sun et al. 2017). To locate the candidate region associated with variations in SL, we performed a microarray analysis between the two DNA pools of the BC_3F_1 generation. Compared to the traditional mapping methods using amplified fragment-length polymorphism analysis, this technique is more efficient and cost-effective. Since rapeseed is an allotetraploid species with numerous homoeologous exchanges, tandemly duplicated repeats, and transposable elements, genomic gaps remain in the reference genomes (Chalhoub et al. 2014; Sun et al. 2017). In the mapping region of *BnSLA09*, a 27.9 kb genomic gap exists in *B. napus* 'Darmor-*bzh*' reference genome, whereas this gap is absent in *B. napus* 'ZS11' reference genome. To fine map and locate the candidate interval rapidly and accurately by the map-based cloning method, it is necessary to consider all reference genome sequences.

Map-based cloning in this study identified a major gene controlling both SL and SW, and sequence and expression analyses indicated that BnaA09g55530D is the putative gene responsible for variations in SL. Fragment replacement and SNP variations found in the upstream region of the candidate gene may alter the expression of this gene and cause variations in SL. The candidate gene may positively regulate SW as well as in the 186 rapeseed accessions identified by the associated markers. Therefore, identification of the silique-related gene and the development of functional markers will enhance the molecular breeding of high-yield rapeseed varieties.

Author contribution statement WS, PQ, and MY performed the experiments; BL carried out the SNP experiment, and ZW designed the SSR and InDel primers. WS analyzed the data and wrote the manuscript. JW, BY, CM, JS, and TF contributed the materials, experiment tools and supervised the study. JT conceived and supervised the writing. All the authors read and approved the final manuscript.

Acknowledgements We sincerely thank Professor Yongming Zhou and Professor Liang Guo for kindly providing the silique length and seed weight data of the 521 accessions. This work was financed by the funding from the National Key Research and Development Program of China (Grant Number 2016YFD0100305).

Compliance with ethical standards

Ethical standard The authors declare that this study complies with current laws of China.

Conflict of interest The authors declare that they have no conflict of interest.

References

Bai XF, Huang Y, Hu Y, Liu HY, Zhang B, Smaczniak C, Hu G, Han ZM, Xing YZ (2017) Duplication of an upstream silencer of *FZP* increases grain yield in rice. Nat Plants 3:885–893

Chae K, Isaacs CG, Reeves PH, Maloney GS, Muday GK, Nagpal P, Reed JW (2012) *Arabidopsis SMALL AUXIN UP RNA63* promotes hypocotyl and stamen filament elongation. Plant J 71:684–697

Chalhoub B, Denoeud F, Liu SY, Parkin IAP, Tang HB, Wang XY, Chiquet J, Belcram H, Tong CB, Samans B, Correa M, Da Silva C, Just J, Falentin C, Koh CS, Le Clainche I, Bernard M, Bento P, Noel B, Labadie K, Alberti A, Charles M, Arnaud D, Guo H, Daviaud C, Alamery S, Jabbari K, Zhao MX, Edger PP, Chelaifa H, Tack D, Lassalle G, Mestiri I, Schnel N, Le Paslier MC, Fan GY, Renault V, Bayer PE, Golicz AA, Manoli S, Lee TH, Thi VHD, Chalabi S, Hu Q, Fan CC, Tollenaere R, Lu YH, Battail C, Shen JX, Sidebottom CHD, Wang XF, Canaguier A, Chauveau A, Berard A, Deniot G, Guan M, Liu ZS, Sun FM, Lim YP, Lyons E, Town CD, Bancroft I, Wang XW, Meng JL, Ma JX, Pires JC, King GJ, Brunel D, Delourme R, Renard M, Aury JM, Adams KL, Batley J, Snowdon RJ, Tost J, Edwards D, Zhou YM, Hua W, Sharpe AG, Paterson AH, Guan CY, Wincker P (2014) Early allopolyploid evolution in the post-Neolithic *Brassica napus* oilseed genome. Science 345:950–953

Chapman MA, Tang S, Draeger D, Nambeesan S, Shaffer H, Barb JG, Knapp SJ, Burke JM (2012) Genetic analysis of floral symmetry in Van Gogh's sunflowers reveals independent recruitment of *CYCLOIDEA* genes in the Asteraceae. PLoS Genet 8:e1002628

Chay P, Thurling N (1989a) Identification of genes controlling pod length in spring rapeseed, *Brassica napus* L, and their utilization for yield improvement. Plant Breed 103:54–62

Chay P, Thurling N (1989b) Variation in pod length in spring rape (*Brassica napus*) and its effect on seed yield and yield components. J Agric Sci 113:139–147

Chen W, Zhang Y, Liu X, Chen B, Tu J, Tingdong F (2007) Detection of QTL for six yield-related traits in oilseed rape (*Brassica napus*) using DH and immortalized F_2 populations. Theor Appl Genet 115:849–858

Clarke WE, Higgins EE, Plieske J, Wieseke R, Sidebottom C, Khedikar Y, Batley J, Edwards D, Meng J, Li R, Lawley CT, Pauquet J, Laga B, Cheung W, Iniguez-Luy F, Dyrszka E, Rae S, Stich B, Snowdon RJ, Sharpe AG, Ganal MW, Parkin IA (2016) A high-density SNP genotyping array for *Brassica napus* and its ancestral diploid species based on optimised selection of single-locus markers in the allotetraploid genome. Theor Appl Genet 129:1887–1899

Diepenbrock W (2000) Yield analysis of winter oilseed rape (*Brassica napus* L.): a review. Field Crops Res 67:35–49

Dong HL, Tan CD, Li YZ, He Y, Wei S, Cui YX, Chen YG, Wei DY, Fu Y, He YJ, Wan HF, Liu Z, Xiong Q, Lu K, Li JN, Qian W (2018) Genome-wide association study reveals both overlapping and independent genetic loci to control seed weight and silique length in *Brassica napus*. Front Plant Sci 9:921. https://doi.org/10.3389/fpls.2018.00921

Fan C, Cai G, Qin J, Li Q, Yang M, Wu J, Fu T, Liu K, Zhou Y (2010) Mapping of quantitative trait loci and development of allele-specific markers for seed weight in *Brassica napus*. Theor Appl Genet 121:1289–1301

Fu Y, Wei D, Dong H, He Y, Cui Y, Mei J, Wan H, Li J, Snowdon R, Friedt W, Li X, Qian W (2015) Comparative quantitative trait loci for silique length and seed weight in *Brassica napus*. Sci Rep 5:14407

Glover NM, Redestig H, Dessimoz C (2016) Homoeologs: what are they and how do we infer them? Trends Plant Sci 21:609–621

Hou JN, Long Y, Raman H, Zou XX, Wang J, Dai ST, Xiao QQ, Li C, Fan LJ, Liu B, Meng JL (2012) A *Tourist*-like MITE insertion in the upstream region of the *BnFLC.A10* gene is associated with vernalization requirement in rapeseed (*Brassica napus* L.). BMC Plant Biol 12:238

Huo X, Wu S, Zhu ZF, Liu FX, Fu YC, Cai HW, Sun XY, Gu P, Xie DX, Tan LB, Sun CQ (2017) *NOG1* increases grain production in rice. Nat Commun 8:1497

Hur YS, Um JH, Kim S, Kim K, Park HJ, Lim JS, Kim WY, Jun SE, Yoon EK, Lim J, Ohme-Takagi M, Kim D, Park J, Kim GT, Cheon CI (2015) *Arabidopsis thaliana* homeobox 12 (ATHB12), a homeodomain-leucine zipper protein, regulates leaf growth by promoting cell expansion and endoreduplication. New Phytol 205:316–328

Ito T, Meyerowitz EM (2000) Overexpression of a gene encoding a cytochrome P450, *CYP78A9*, induces large and seedless fruit in Arabidopsis. Plant Cell 12:1541–1550

Khan F, Ali S, Shakeel A, Saeed A, Abbas G (2006) Correlation analysis of some quantitative characters in *Brassica napus* L. J Agric Res 44:7–14

King SP, Lunn JE, Furbank RT (1997) Carbohydrate content and enzyme metabolism in developing canola siliques. Plant Physiol 114:153–160

Kolovos P, Knoch TA, Grosveld FG, Cook PR, Papantonis A (2012) Enhancers and silencers: an integrated and simple model for their function. Epigenet Chromatin 5:1

Kong Y, Zhu Y, Gao C, She W, Lin W, Chen Y, Han N, Bian H, Zhu M, Wang J (2013) Tissue-specific expression of *SMALL AUXIN UP RNA41* differentially regulates cell expansion and root meristem patterning in Arabidopsis. Plant Cell Physiol 54:609–621

Kosambi DD (1944) The estimation of map distances from recombination values. Ann Eugen 12:172–175

Li N, Shi J, Wang X, Liu G, Wang H (2014) A combined linkage and regional association mapping validation and fine mapping of two major pleiotropic QTLs for seed weight and silique length in rapeseed (*Brassica napus* L.). BMC Plant Biol 14:114

Li W, Zhu Z, Chern M, Yin J, Yang C, Ran L, Cheng M, He M, Wang K, Wang J, Zhou X, Zhu X, Chen Z, Wang J, Zhao W, Ma B, Qin P, Chen W, Wang Y, Liu J, Wang W, Wu X, Li P, Wang J, Zhu L, Li S, Chen X (2017) A natural allele of a transcription factor in rice confers broad-spectrum blast resistance. Cell 170:114.e15–126.e15

Li N, Song D, Peng W, Zhan J, Shi J, Wang X, Liu G, Wang H (2018) Maternal control of seed weight in rapeseed (*Brassica napus* L.): the causal link between the size of pod (mother, source) and seed (offspring, sink). Plant Biotechnol J 1:1. https://doi.org/10.1111/pbi.13011

Liu RH, Meng JL (2003) MapDraw: a microsoft excel macro for drawing genetic linkage maps based on given genetic linkage data. Hereditas 25:317–321

Liu J, Hua W, Hu Z, Yang H, Zhang L, Li R, Deng L, Sun X, Wang X, Wang H (2015) Natural variation in *ARF18* gene simultaneously affects seed weight and silique length in polyploid rapeseed. Proc Natl Acad Sci USA 112:E5123–E5132

Liu S, Fan C, Li J, Cai G, Yang Q, Wu J, Yi X, Zhang C, Zhou Y (2016) A genome-wide association study reveals novel elite allelic variations in seed oil content of *Brassica napus*. Theor Appl Genet 129:1203–1215

Murray MG, Thompson WF (1980) Rapid isolation of high molecular weight plant DNA. Nucleic Acids Res 8:4321–4325

Østergaard L, King GJ (2008) Standardized gene nomenclature for the *Brassica genus*. Plant Methods 4:10

Porto MS, Pinheiro MP, Batista VG, dos Santos RC, Filho Pde A, de Lima LM (2014) Plant promoters: an approach of structure and function. Mol Biotechnol 56:38–49

Rossato L, Laine P, Ourry A (2001) Nitrogen storage and remobilization in *Brassica napus* L. during the growth cycle: nitrogen fluxes within the plant and changes in soluble protein patterns. J Exp Bot 52:1655–1663

Sadat HA, Nematzadeh GA, Jelodar NB, Chapi OG (2010) Genetic evaluation of yield and yield components at advanced generations in rapeseed (*Brassica napus* L.). Afr J Agric Res 5:1958–1964

Samizadeh H, Samadi BY, Behamta M, Taleii A, Stringam G (2007) Study of pod length trait in doubled haploid *Brassica napus* population by molecular markers. J Agric Sci 9:129–136

Shi J, Li R, Qiu D, Jiang C, Long Y, Morgan C, Bancroft I, Zhao J, Meng J (2009) Unraveling the complex trait of crop yield with quantitative trait loci mapping in *Brassica napus*. Genetics 182:851–861

Sotelo-Silveira M, Cucinotta M, Chauvin AL, Montes RAC, Colombo L, Marsch-Martinez N, de Folter S (2013) Cytochrome P450 *CYP78A9* is involved in arabidopsis reproductive development. Plant Physiol 162:779–799

Sun F, Fan G, Hu Q, Zhou Y, Guan M, Tong C, Li J, Du D, Qi C, Jiang L, Liu W, Huang S, Chen W, Yu J, Mei D, Meng J, Zeng P, Shi J, Liu K, Wang X, Wang X, Long Y, Liang X, Hu Z, Huang G, Dong C, Zhang H, Li J, Zhang Y, Li L, Shi C, Wang J, Lee SM, Guan C, Xu X, Liu S, Liu X, Chalhoub B, Hua W, Wang H (2017) The high-quality genome of *Brassica napus* cultivar 'ZS11' reveals the introgression history in semi-winter morphotype. Plant J 92:452–468

Udall JA, Quijada PA, Lambert B, Osborn TC (2006) Quantitative trait analysis of seed yield and other complex traits in hybrid spring rapeseed (*Brassica napus* L.): 2. Identification of alleles from unadapted germplasm. Theor Appl Genet 113:597–609

Van Ooijen JW (2006) JoinMap® 4.0: software for the calculation of genetic linkage maps in experimental populations. Kyazma BV, Wageningen

Wang X, Chen L, Wang A, Wang H, Tian J, Zhao X, Chao H, Zhao Y, Zhao W, Xiang J, Gan J, Li M (2016) Quantitative trait loci analysis and genome-wide comparison for silique related traits in *Brassica napus*. BMC Plant Biol 16:71

Xia SQ, Cheng L, Zu F, Dun XL, Zhou ZF, Yi B, Wen J, Ma CZ, Shen JX, Tu JX, Fu TD (2012) Mapping of *BnMs4* and *BnRf* to a common microsyntenic region of *Arabidopsis thaliana* chromosome 3 using intron polymorphism markers. Theor Appl Genet 124:1193–1200

Xu L, Hu K, Zhang Z, Guan C, Chen S, Hua W, Li J, Wen J, Yi B, Shen J, Ma C, Tu J, Fu T (2016) Genome-wide association study reveals the genetic architecture of flowering time in rapeseed (*Brassica napus* L.). DNA Res 23:43–52

Yang P, Shu C, Chen L, Xu J, Wu J, Liu K (2012) Identification of a major QTL for silique length and seed weight in oilseed rape (*Brassica napus* L.). Theor Appl Genet 125:285–296

Zhang L, Yang G, Liu P, Hong D, Li S, He Q (2011) Genetic and correlation analysis of silique-traits in *Brassica napus* L. by quantitative trait locus mapping. Theor Appl Genet 122:21–31

Zhao X, Li B, Zhang K, Hu K, Yi B, Wen J, Ma C, Shen J, Fu T, Tu J (2016) Breeding signature of combining ability improvement revealed by a genomic variation map from recurrent selection population in *Brassica napus*. Sci Rep 6:29553

Zhou ZF, Dun XL, Xia SQ, Shi DY, Qin MM, Yi B, Wen J, Shen JX, Ma CZ, Tu JX, Fu TD (2012) *BnMs3* is required for tapetal differentiation and degradation, microspore separation, and pollen-wall biosynthesis in *Brassica napus*. J Exp Bot 63:2041–2058